Keeping the Team Moving: Resilient Multi-Robot Coordination for Effective Human–Robot Collaboration

Anonymous Author(s)

Abstract

Safe and resilient multi-robot collaboration in human environments is a critical challenge for real world deployment. While persistent and extensive work is being carried out on human following, existing methods often rely on idealized assumptions of perfect perception and localization. Consequently, they fail to address catastrophic failures like controller deadlocks in cluttered spaces, causing interactional breakdowns that halt the team's progress and compromise task success. In this work, we tackle these challenges by introducing a safety aware control architecture built on two core ideas that enables resilient human-robot teaming. We have developed a robust perception pipeline that reliably estimates human position from noisy, ambiguous RF-ranging data. This is achieved using a two-phased spatiotemporal filter that transforms sparse sensor measurements into a continuous human position estimate, even with a minimal two robot configuration. We then present a multi-layered failsafe supervisor that monitors the low level MPC and uses a dual trigger mechanism monitoring the system costs and the progress disparity. When deadlock is detected, a progress aware recovery planner ensures that the system's mobility is restored and the formation is guided safely out of the trap. We demonstrate that our architecture successfully navigates complex trap scenarios where nominal planners fail, demonstrating a significant improvement in system endurance, reliability and robustness.

Keywords

Shared autonomy, Bi-directional communication, Cooperative transport, Multi-Robot System, Human-in-the-Loop

ACM Reference Format:

Anonymous Author(s). 2025. Keeping the Team Moving: Resilient Multi-Robot Coordination for Effective Human–Robot Collaboration. In . ACM, New York, NY, USA, 9 pages. https://doi.org/10.1145/nnnnnnn.nnnnnnn

1 Introduction

Imagine a multi-robot team collaboratively transporting a large, fragile object alongside a human through a cluttered environment, when it suddenly freezes at a critical point without any explanation. This moment of failure is more than a technical glitch; it halts the team's progress, jeopardizes the collaborative task, and can introduce significant safety risks. Overcoming such deadlocks is a critical challenge for the real-world deployment of robotic systems in collaborative environments where humans and robots share workspaces. Human-robot collaboration (HRC) aims to establish synergistic partnerships that leverage the unique strengths of both humans—such as advanced reasoning, dexterity, and adaptability—and robots, which offer superior strength, precision, and endurance [1]. Envisioning scenarios that once seemed unreal, like a pair of robots cooperatively carrying a large, fragile object alongside a human through a cluttered environment, as depicted in Fig. 1, involves the primary task of the multi-robot system to competently track and follow or accompany the human through dynamic workspaces [6]. For successful implementation of these systems, prioritizing safety as much as efficiency is essential. This can be obtained through a collaborative framework based on an uncompromising guarantee of human safety [8].

This work investigates cooperative object transport involving a human and a team of mobile robots. The human specifies the overall motion, while the robots regulate their trajectories to maintain coordination. The interaction is bidirectional where the robots can communicate feedback to the human, including requests to adjust speed in constrained environments and notifications of planner failures. This makes the robot team's behavior more understandable, accessible and transparent to its human partner. Such feedback mechanisms promote adaptive synchronization between agents, thereby improving the reliability and efficiency of the transport task and creating a more cohesive shared partnership. To achieve robust tracking, human carries a non-line-of-sight, RF ranging tracker (e.g., Ultra-Wideband), and each robot estimates its distance to the human via multilateration.

The overall problem is to develop a control architecture that can foster safe and efficient partnership by enabling the robotic team to adapt to a wide range of situations. The core objective is that this adaptation is made requiring as minimal changes as possible, thereby minimizing the cognitive load on the human partner, while:

(1) Reliably estimating the human's state from noisy and potentially ambiguous sensor data.
(2) Maintaining the object-carrying formation.
(3) Proactively avoiding collisions with all static and dynamic obstacles using Velocity Obstacle methods incorporated within the MPC framework.
(4) Maintaining a predictable and comfortable distance from the human, respecting their personal safety space and to prevent potential collisions.
(5) Possessing the intelligence to detect and gracefully recover from its own planning failures, minimizing disruption to the collaborative task through proactive bi-directional communication.

Model Predictive Control (MPC) has emerged as a leading strategy for safe robot behaviour due to its capability to plan future actions while adhering to strict constraints [2],[9]. However, the effectiveness of MPC is fundamentally dependent on the reliability

Conference'17, Washington, DC, USA

ACM ISBN 978-x-xxxx-xxxx-x/YYYY/MM
https://doi.org/10.1145/nnnnnnn.nnnnnnn

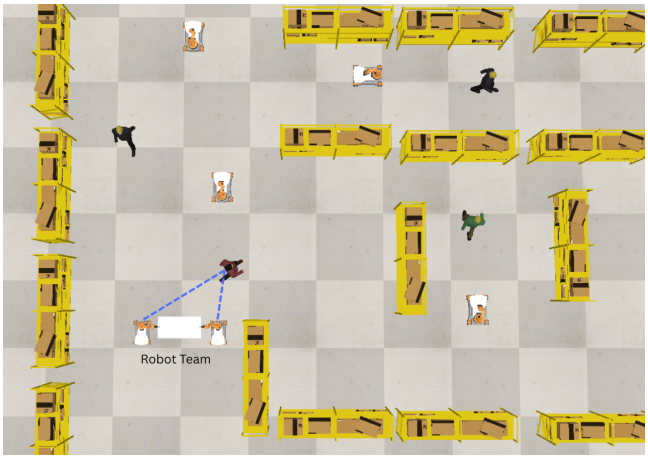

Figure 1: Illustrating the complexity of human-robot cooperative transport in a shared, dynamic workspace. A mobile manipulator team navigates an object through a cluttered environment while maintaining formation, ensuring safety around dynamic human co-workers and recovering from planning failures.

of its input data and predictions [3]. For MPC to be effective in Human Robot Interaction (HRI), the abstract concept of "safety" must be incorporated into precise mathematical equations of objectives and constraints. Recent work has focused on defining social space constraints [10] and explicitly accounting for human behavioral uncertainties within the prediction model [5, 7]. While modeling human uncertainty is a critical first step, the next frontier and the focus of this work is to empower the robot to move beyond this modeling to act on uncertainty in a principled, risk-aware manner. While these approaches advance socially-aware control, they do not explicitly address perception failures from sensor noise and ambiguity, nor provide mechanisms for detecting and recovering from controller failures which are both important for safety-critical collaborative transport.

Lacking robustness against real-world unpredictability is the primary barrier to safety, as a robot susceptible to failures at both the perception and control levels becomes not just ineffective, but a significant safety liability when it cannot reliably perceive its human partner or recover from planning failures. Relying solely on dominant sensing techniques like vision and LiDAR for example, introduces a significant point of failure. This is due to occlusions, identity confusion in crowded scenes, variable lighting conditions and blind spots in obstacle-prone areas [4] that can cause critical loss of human's state data. These failures endanger the human by compromising the system's overall safety in critical applications. Radio frequency (RF) technologies like Ultra-Wideband (UWB) present a compelling alternative [12], offering centimeter level accuracy via multilateration while being inherently robust from occlusions and adverse lighting conditions. It also offers non line of sight (NLOS) capabilities and provides unambiguous digital identity, making it a superior choice for safety critical applications.

However, even robust RF sensors introduce their own set of challenges. Firstly, raw measurements received from the sensors are corrupted by noise, which can render the geometric intersection problem causing difficulties in finding the exact position and thus leading to localization failures. Secondly, in minimalist formation configuration like a two robot team, multilateration yields a critical issue: producing two distinct human position estimates. Without a strong and solid method to resolve these ambiguities, the system cannot generate a reliable control signal. Beyond perception challenges, the robot's own planner is susceptible to failures in complex environments. This failure can cause the robot to behave erratically or stop suddenly, making it completely unpredictable for the human partner. This leads to a "collaboration gap" and breach of trust, which undermines the human-robot team and thereby leaves the human confused and uncertain of what to do next.

To address these critical gaps in both the perceptual uncertainty and control, we propose a hierarchical, multi-layered architecture for safe and robust multi-robot human following. Our primary contributions are:

(1) An end-to-end pipeline for risk-aware planning that transforms raw sensor data into predictable robot behavior. Our contribution begins with a robust perception pipeline that transforms noisy and ambiguous measurements from RF ranging technologies like UWB into a reliable human state estimate. This pipeline is resilient to sensor noise by defining a "Region of Plausibility" and is capable of resolving ambiguities in human position estimation that arise in a two-robot setup. Building on this foundation, we then feed this reliable state estimate into a context-aware probabilistic predictor to forecast a full distribution of the human's likely future paths. This entire uncertainty-aware forecast is then used by a Stochastic MPC to produce safe, predictable, and cautiously adaptive robot behavior.
(2) A multi-layered, shared autonomy protocol designed to initiate a human-in-the-loop resolution process when a planning failure occurs. This protocol is activated by a dual-trigger failsafe supervisor that detects "coordination gaps," such as when the robot falls behind or gets stuck. When the robot team struggles instead of simply executing a pre-planned escape, it proactively communicates its state to the human partner, offering a set of strategic choices to resolve the situation together. This turns a potential point of failure and frustration into a moment of resilience, making the robot a more viable and trustworthy partner for everyday tasks.

The remainder of this paper is structured as follows: Section 2 presents the detailed formulation of our hierarchical architecture for robust perception pipeline and the risk-aware S-MPC. Section 3 details the shared autonomy protocol. Section 4 details the experimental validation, demonstrating how our integrated system produces safer, more predictable behavior and enables effective human-robot collaboration. Finally, Section 5 concludes the paper and discusses future work.

2 System Architecture: Perception, Prediction, and Risk-Aware Planning

The architecture of our collaborative system shown in Fig. 2, is present to ensure safe and reliable human collaboration with multiple robots, especially when controller failure and perceptual ambiguities arise. It consists of two essential modules: a *Perception*

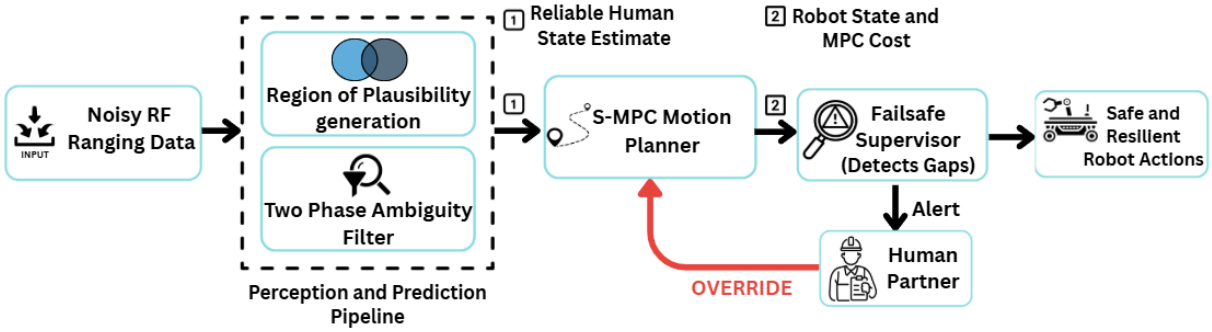

Figure 2: An overview of the proposed control architecture. (Input) Noisy RF-ranging data is first processed by the Perception and Prediction Pipeline, which uses a Region of Plausibility generator and a Two-Phase Ambiguity Filter. (1) This produces a reliable human state estimate that is fed to the S-MPC Motion Planner. (2) In parallel, a Failsafe Supervisor monitors the robot's state and MPC cost to detect coordination gaps. Upon detection, it alerts the Human Partner, who can issue an OVERRIDE command to collaboratively resolve the issue, leading to Safe and Resilient Robot Actions.

and Prediction Module that transforms noisy sensor data into a probabilistic forecast of the human's future path and a *Risk-Aware Motion Planner* that uses this forecast to generate safe, adaptive and resilient robot operations.

2.1 Foundational Perception: From Raw Data to a Reliable State Estimate

The foundational basis of a safe Human Robot Interaction system has a very major dependency on the perceived human inputs. Our pipeline is designed to remain reliable even under sensor noise and geometric ambiguities underlying in minimal settings. Here the concept of *multilateration* is used to calculate accurate human position. It is a well known geometric method for determining the position of a point by measuring its distance from multiple known reference points. Our system defines the localization problem space as a 2D horizontal projection, tailored for operation within planar ground surfaces. While UWB sensors provide 3D range data, we leverage the consistent height difference (Δz) between the sensors mounted on the robots and the human-worn sensor. This environmental constraint allows us to accurately calculate 2D projected distances for subsequent annular intersection calculations. This approach enables robust localization within the defined operational space.

2.1.1 Concept of the Region of Plausibility. To handle the noisy distance measurements received from RF ranging sensors, the raw or noisy data points are transformed into a stable and high-confidence area. We model the plausible location of the human relative to each robot not as a circle but as an annulus (a ring). This is attained by defining a buffer radius, r_{buffer}. This is calculated based on the standard deviation of the measurement error, $\sigma_{\textbf{sensor}}$, determined empirically for the sensor. The buffer is rigorously defined as $r_{\textbf{buffer}} = 3\sigma_{\textbf{sensor}}$, creating a 99.7% confidence interval around each measurement. The final "Region of Plausibility" as illustrated in Figure 3 is the geometric intersection of these annuli, which guarantees that a valid solution area exists even when noise would prevent simple circles from intersecting.

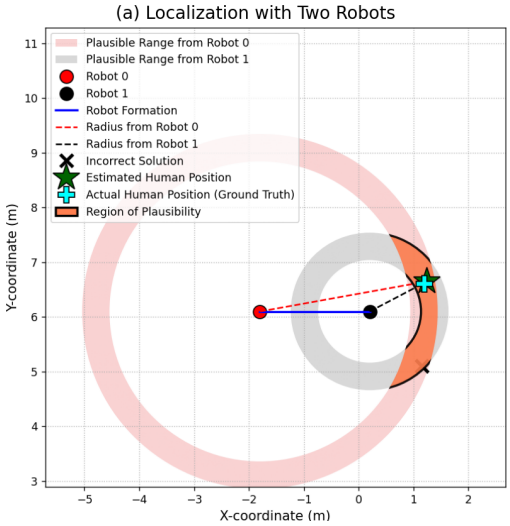

Figure 3: Visualization of the Region of Plausibility concept. The noisy distance measurements from Robot 0 (red) and Robot 1 (black) are modeled as annuli (the shaded pink and grey rings) rather than simple radii. The geometric intersection of these annuli forms the final, robust 'Region of Plausibility' (shown in orange), which contains the true human position.

2.1.2 The Two-Phase Ambiguity Resolution Filter. A critical issue with a two-robot setup is that the intersection of their data results in two distinct locations for the human. Our filter resolves this ambiguity in two phases as can be seen in detail in Figure 4.

- *Initialization (t=0):* With no prior motion history, we use the task's geometric context to bootstrap the filter. We define a "front vector" $\mathbf{v}_{\text{front}}$, based on the formation's initial orientation. The initial estimate, $\hat{\mathbf{p}}_h(0)$, is chosen by selecting the candidate centroid, $\mathbf{c}$, that is most aligned with this vector, calculated as

$$\hat{\mathbf{p}}_h(0) = \text{argmax}_{\mathbf{c}\in\{\mathbf{c}_A,\mathbf{c}_B\}}((\mathbf{c} - \mathbf{p}_{\text{mid}}) \cdot \mathbf{v}_{\text{front}}) \quad (1)$$

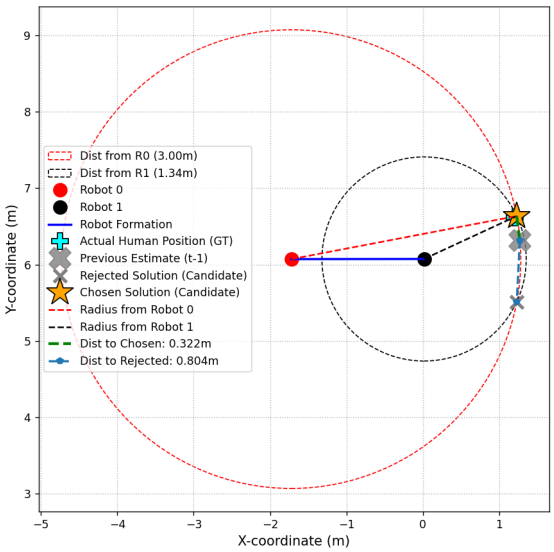

Figure 4: The Ambiguity Resolution process at a single time step. The two potential locations (candidates) are the intersections of the red and black distance circles. The filter compares the displacement from the Previous Estimate (t-1) to both the Chosen Solution (green path, 0.322m) and the Rejected Solution (blue path, 0.804m). By selecting the candidate with the minimum displacement, the filter correctly identifies the true human trajectory.

where $\mathbf{p}_{\text{mid}}$ is the formation's midpoint and $\mathbf{c}_A$ and $\mathbf{c}_B$ are the centroids of the two candidate regions for the human's location derived from multilateration.

- *Continuous Tracking ($t > 0$):* For all subsequent timesteps, we apply the Minimum Displacement Principle. Leveraging the physical C^0 continuity of human motion, the new estimate $\hat{\mathbf{p}}_h(t)$ is selected as the candidate centroid from the current timestep $\mathbf{c}(t)$, that is closest to the previous estimate, $\hat{\mathbf{p}}_h(t-1)$:

$$\hat{\mathbf{p}}_h(t) = \underset{\mathbf{c}(t)\in\{\mathbf{c}_A(t),\mathbf{c}_B(t)\}}{\operatorname{argmin}} \|\mathbf{c}(t) - \hat{\mathbf{p}}_h(t-1)\| \tag{2}$$

While this filter is specifically designed for the challenging two-robot case, its underlying principles suggest a path toward robust perception in larger teams. In scenarios with three or more robots, the Minimum Displacement Principle could serve as a powerful tool for outlier rejection, enforcing temporal consistency to discard a false "ghost" solution caused by a faulty sensor. This indicates potential for graceful degradation; if a sensor on a robot in a larger team fails, the system may temporarily revert to the two-robot case, which our filter is explicitly designed to handle.

2.2 Context-Aware Probabilistic Prediction

To plan safe and socially intelligent actions, a robot needs to do more than just know where its human partner is right now. A single point-estimate is insufficient for this kind of forward-looking, risk-aware planning. Therefore, the next crucial step in our pipeline is to transform the reliable state estimate from our foundational perception module into a rich, probabilistic forecast of the human's future movement.

To achieve this, we employ a Particle Filter. We represent the human's state at time t by a vector $\mathbf{x}_t = [\mathbf{p}_h(t), \mathbf{v}_h(t)]$, which includes their 2D position and velocity. The particle filter approximates the distribution over this state with a set of M weighted particles $\{\mathbf{x}_t^{(i)}, w_t^{(i)}\}_{i=1}^{M}$. At each prediction step, a new set of particles is generated by propagating each particle from the previous step through our context-aware motion model:

$$\mathbf{x}_t^{(i)} \sim p(\mathbf{x}_t|\mathbf{x}_{t-1}^{(i)}, \mathcal{M}) \tag{3}$$

where $\mathbf{x}_t^{(i)}$ is the newly predicted state for the i-th particle, sampled from a probabilistic motion model $p(\cdot)$. Crucially, this model is conditioned not only on the particle's previous state $\mathbf{x}_{t-1}^{(i)}$ but also on the environment map $\mathcal{M}$. This conditioning ensures that predicted paths are kinematically feasible and are highly unlikely to pass through known obstacles, embedding environmental context directly into our forecast. To model the uncertainty inherent in human behavior, we also add random noise to each particle's velocity at every prediction step.

The final output of this stage is not a single path, but a "tube" of particle clouds—a set of particles for each of the H time steps in the prediction horizon. The subsequent planning module (S-MPC) directly uses this particle tube to calculate expected risk, effectively implementing a chance constraint that scales with the predicted uncertainty of the forecast. This rich, context-aware forecast provides the subsequent planning module with a complete picture of the human's potential future movements, a significant improvement over the brittle constant velocity models that often lead to reactive or unsafe robot behavior.

2.3 The Stochastic MPC: Risk-Aware Motion Planning

Our approach moves beyond a traditional deterministic MPC, which operates under the assumption of perfect knowledge and simply tracks a single reference path. This framework reasons about the full distribution of uncertainty captured in the particle clouds from the previous section 2.2, allowing it to manage risk in a principled way. The S-MPC minimizes a total cost function J over a prediction horizon H by solving an optimal control problem using CasADi with the IPOPT solver.

2.3.1 The Hybrid Objective Function. The S-MPC's objective is to minimize a total cost which combines standard tracking objectives with a probabilistic risk assessment. The control goal is to find the optimal control sequence $\mathbf{u}^*$ that minimizes the total cost over the horizon H:

$$\mathbf{u}^* = \underset{\mathbf{u}}{\operatorname{argmin}} \sum_{k=0}^{H-1} \left(J_{\text{deterministic},k} + J_{\text{stochastic},k}\right) \tag{4}$$

The stage cost is composed of two primary parts: a deterministic cost component $J_{\text{deterministic},k}$ and a stochastic cost component $J_{\text{stochastic},k}$. The deterministic part maintains formation integrity and tracks a single reference path $\mathbf{p}_{\text{ref}}(k)$. **This reference path is derived from the human's high-level path planner by offsetting the desired formation center from the mean of the predicted particle cloud along the path by a safe distance**

$D_{\textbf{safe}}$. This component includes standard terms for control effort, rate of change of control, and tracking error:

$$J_{\text{deterministic},k} = |\mathbf{u}_k|^2_{\mathbf{W}_u} + |\mathbf{u}_k - \mathbf{u}_{k-1}|^2_{\mathbf{W}_{\text{rate}}} + |\mathbf{p}_{\text{com}}(k) - \mathbf{p}_{\text{ref}}(k)|^2_{\mathbf{W}_e} + |e_k^{\text{form}}|^2_{w_f} \tag{5}$$

The stochastic cost component, $J_{\text{stochastic},k}$, is detailed in Section 2.3.2, where it directly penalizes risk based on the full particle distribution.

2.3.2 The Core Safety Mechanism: Probabilistic Risk Cost. The key to the S-MPC's risk-aware behavior is the implementation of a "probabilistic risk cost term". Instead of a hard constraint that states "distance > D_{safe}," we formulate safety as a cost term that penalizes potential collisions based on the expected value of risk over all possible human paths. This cost term ensures that the robot prioritizes safety strongly, while maintaining solver feasibility by allowing minor, penalized violations if necessary.

We approximate the probability of collision by evaluating the expected risk across the particles from our forecast. At each timestep k in the plan, we define the stochastic cost term $J_{\text{stochastic},k}$ as follows:

$$J_{\text{stochastic},k} = Q_{\text{risk}} \cdot \mathbb{E}[\max(0, R^2_{\text{total}} - |\mathbf{p}_{\text{com}}(k) - \mathbf{p}_h^{(i)}(k)|^2)] \tag{6}$$

where R_{total} represents the total required separation distance, and the expectation $\mathbb{E}[\cdot]$ is approximated by summing the risk cost over the M particles in the cloud:

$$J_{\text{stochastic},k} \approx \frac{Q_{\text{risk}}}{M} \sum_{i=1}^{M} \max(0, R^2_{\text{total}} - |\mathbf{p}_{\text{com}}(k) - \mathbf{p}_h^{(i)}(k)|^2) \tag{7}$$

This formulation leads to emergent cautious behavior. When prediction uncertainty is high (e.g., the particle cloud is large and spread out), the expected risk term $J_{\text{stochastic},k}$ increases significantly. To minimize this increased cost, the S-MPC plans a more conservative path for the robot (e.g., slowing down or taking a wider arc). The robot's caution is not explicitly programmed; it is the mathematical result of minimizing the expected penalty cost in the face of uncertainty.

2.3.3 Dynamic Obstacle Avoidance via Velocity Obstacles. Our MPC framework directly integrates the Velocity Obstacle (VO) method [11] for avoiding both static and dynamic obstacles. For each obstacle, the VO defines the set of all relative velocities that will result in a collision. We use the concept of Signed Minimum Distance (smd) to formulate this as a nonlinear constraint, ensuring the "smd" between the robot formation and each obstacle remains non-negative:

$$\text{smd}(\mathbf{p}_f, \mathbf{v}_f, \mathbf{p}_o, \mathbf{v}_o, r_f, r_o) \geq 0 \tag{8}$$

where $(\mathbf{p}_f, \mathbf{v}_f, r_f)$ are the formation's state and radius, and $(\mathbf{p}_o, \mathbf{v}_o, r_o)$ are the obstacle's predicted state and radius. This is implemented as a constraint at every time step k within the horizon, allowing the MPC to proactively generate guaranteed collision-free velocities.

3 Shared Autonomy for Collaborative Recovery

3.1 Triggering the Protocol: Detecting Coordination Gaps

The shared autonomy protocol is not continuously active, it is initiated by a supervisory layer that continuously monitors the team's performance. This supervisor uses a dual-trigger logic to identify two distinct types of failures that can lead to a breakdown in collaboration.

3.1.1 Trigger 1: Robot State Failure (Internal Deadlocks). This trigger detects scenarios where the robot team struggles to find a valid motion plan or gets completely stuck in a local minimum. These internal deadlocks represent a complete failure of the autonomous system's ability to navigate or maintain formation. We identify two specific sub-conditions for this failure:

High-Effort Failure ($D_{\textbf{cost}}$): This proactively detects when the MPC is operating under persistently high risk or high cost due to conflicting constraints. To distinguish a high-cost state from a valid, transient cost spike, our logic monitors the median cost over a time window. A high-effort state, D_{cost}, is flagged if this median cost persistently exceeds a severe threshold, τ_{severe}, or if a high percentage of costs in the history exceed a sustained threshold, $\tau_{\text{sustained}}$. This is formally expressed as:

$$D_{\text{cost}} = (\text{median}\{J_{t-N_w:t}\} > \tau_{\text{severe}}) \vee (\text{frac}\{J_k > \tau_{\text{sustained}}\} \geq P_{\text{sus}}) \tag{9}$$

Low-Effort Failure ($D_{\textbf{prog}}$): This detects insidious failures where the MPC has converged to a sub-optimal state, where it remains unproductive (e.g., stuck in a local minimum with low cost). This trigger is only active when the task context, C_{task}, requires motion (e.g., the human is moving or tracking error is high). If motion is required, a low-effort failure, D_{prog}, is flagged if the forward progress along the reference path, $d_{\text{prog}}(t)$, is negligible over the time window:

$$D_{\text{prog}} = 1 \quad \text{if} \quad (C_{\text{task}} = \text{true}) \wedge (d_{\text{prog}}(t) < \tau_p) \tag{10}$$

where τ_p is a small progress threshold.

3.1.2 Trigger 2: Team Coordination Gap (D_{gap}). This trigger detects situations where the robot system's internal state may appear healthy (low cost, or moving slowly), but the collaborative objective is failing due to a growing separation from the human partner. This typically occurs when the human leader's speed or path choice exceeds the robot's ability to maintain pace due to high risk aversion from the S-MPC or navigating complex obstacles.

A coordination gap, D_{gap}, is flagged if the separation distance between the robot formation and the human exceeds a maximum threshold (D_{max}) AND the robots' velocity towards the human is below a minimum threshold (v_{min}) over a sustained time window:

$$D_{\text{gap}} = 1 \quad \text{if} \quad (\|\mathbf{p}_{\text{com}} - \mathbf{p}_h\| > D_{\text{max}}) \wedge (v_{\text{com\_to\_h}} < v_{\text{min}}) \tag{11}$$

This trigger ensures that the system proactively recognizes when the collaboration objective is jeopardized, prompting a necessary human-in-the-loop intervention to maintain task continuity.

3.2 The Collaborative Resolution Protocol

The core contribution of our system is the transition from fully autonomous recovery to a collaborative resolution protocol. Once a coordination gap or deadlock condition is detected by the supervisor (as defined in Section 3.1), the robot system initiates a structured human-in-the-loop process to jointly solve the problem.

3.2.1 Robot-Initiated Communication. Upon detection of a triggering event ($D_{\text{cost}} \vee D_{\text{prog}} \vee D_{\text{gap}} = 1$), the robot system's first action is to provide clear and actionable feedback to the human partner via the wearable device. The nature of the communication is tailored to the specific type of failure detected:

- **High-Effort Deadlock (D_{cost}) or Coordination Gap (D_{gap}):** The system sends a "Warning: High-Effort Maneuver Ahead" signal. This alert, combined with the robot's visible reduction in speed, informs the human that the system is struggling to maintain pace or navigate a complex constraint, prompting a potential adjustment from the human.
- **Low-Effort Deadlock (D_{prog}):** The system sends a distinct "Alert: Planner Stagnation Detected" signal. This notifies the human that the robot has stopped making progress and requires immediate intervention to proceed.

When a coordination issue is detected, the system empowers the human partner by offering three strategic choices. The human can either pause and have the robots catch up ("Wait Mode"), assign a new destination for the robots to navigate to on their own ("Redirection Mode"), or command the robots to take the lead through a difficult area ("Role Reversal Mode"). This shifts the interaction from simple following to active collaboration, using the human's high-level guidance to overcome challenges. This transparent, data-driven feedback transforms the interaction from a passive leader-follower model to an active partnership, allowing the human to understand the robot's challenges and participate in a collaborative solution.

3.3 Executing the Collaborative Plan

Once the human partner selects a strategic option from the Collaborative Resolution Protocol (Section 3.2), the system translates this high-level decision into a specific low-level command for the Stochastic MPC to execute. This ensures that the human's intent is immediately integrated into the robot's planning framework.

3.3.1 Executing "Wait Mode". If the human chooses "Wait Mode," the system temporarily modifies the objective function of the S-MPC. The original tracking cost, J_{track}, which attempts to match the human's full predicted trajectory, is either disabled or replaced. A new, rendezvous-focused cost function is introduced that heavily penalizes the distance to the now stationary human's last known position, $\mathbf{p}_h(t)$, as its primary objective. The probabilistic risk cost (J_{risk}) remains active to ensure that the robot's path to the human is safe, even in cluttered environments.

3.3.2 Executing "Redirection Mode". When the human provides a new goal waypoint, $\mathbf{p}_{\text{new\_goal}}$, the system generates a new reference path. The $\mathbf{p}_{\text{new\_goal}}$ is passed to a high-level path planner (such as A*) to generate a collision-free reference path, $\mathbf{p}_{\text{ref}}(k)$. This new reference path then replaces the old one in the S-MPC's tracking cost term, and the robot proceeds autonomously to execute this new trajectory.

3.3.3 Executing "Role Reversal Mode". If the human selects "Role Reversal Mode," the robot system calculates and executes an optimal, risk-aware path through the difficult area. The S-MPC's objective function (and chance constraint) are used to compute this trajectory, $\mathbf{p}_{\text{robot\_path}}(k)$, ensuring safe navigation. This calculated path is then communicated back to the human (e.g., via a visual representation on the wearable device or through an auditory cue), allowing the human to follow the robot system as it leads through the challenging section.

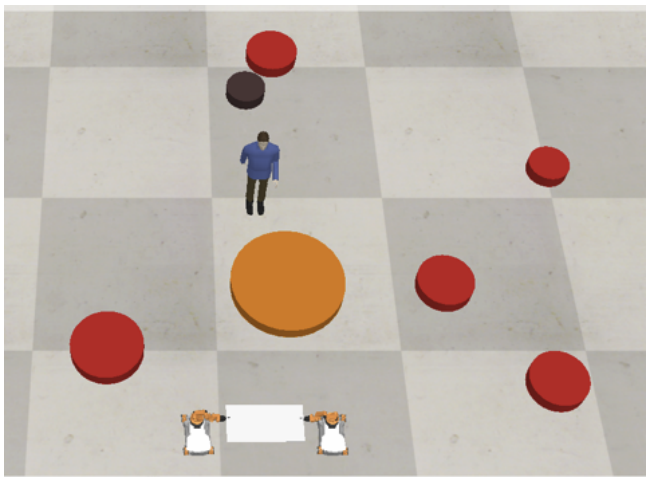

Figure 5: The CoppeliaSim experimental environment. The setup consists of a two-robot formation (KUKA youBots) collaboratively transporting an object, a human model to be followed, and various static obstacles (red and orange cylinders) that create challenging navigation scenarios.

4 EXPERIMENTAL VALIDATION

To validate the performance of our proposed hierarchical architecture for shared autonomy, we conducted a series of experiments in a simulated dynamic environment. The experiments were designed to demonstrate how the system handles uncertainty and transitions to a collaborative mode when facing coordination gaps.

All experiments were carried out in CoppeliaSim, a physics-based simulation environment, as shown in Figure 5. The simulations involve a multi-robot team of two mobile holonomic KUKA youBot robots collaboratively transporting an object. A human model executes collaborative tasks in the environment. We preloaded a map of the scene and generated human trajectories using Voronoi partitioning and A* algorithm, ensuring the robot formation has no prior knowledge of the human's exact path. We modeled an RF-ranging sensor system and simulated noise by adding zero-mean Gaussian noise to the ground-truth distance measurements, using standard deviation (σ) empirically determined from typical hardware specifications.

For all experiments, our proposed system is compared against a *"Baseline MPC"* controller. The baseline represents a deterministic MPC controller without a failsafe supervisor or bi-directional communication protocol, allowing us to evaluate the direct impact of our contributions on system resilience and collaboration.

4.1 Experiment 1: Perception Pipeline and Probabilistic State Estimation Validation

This experiment validates the claim that our proposed two-phased perception pipeline can provide a reliable state estimate, even with

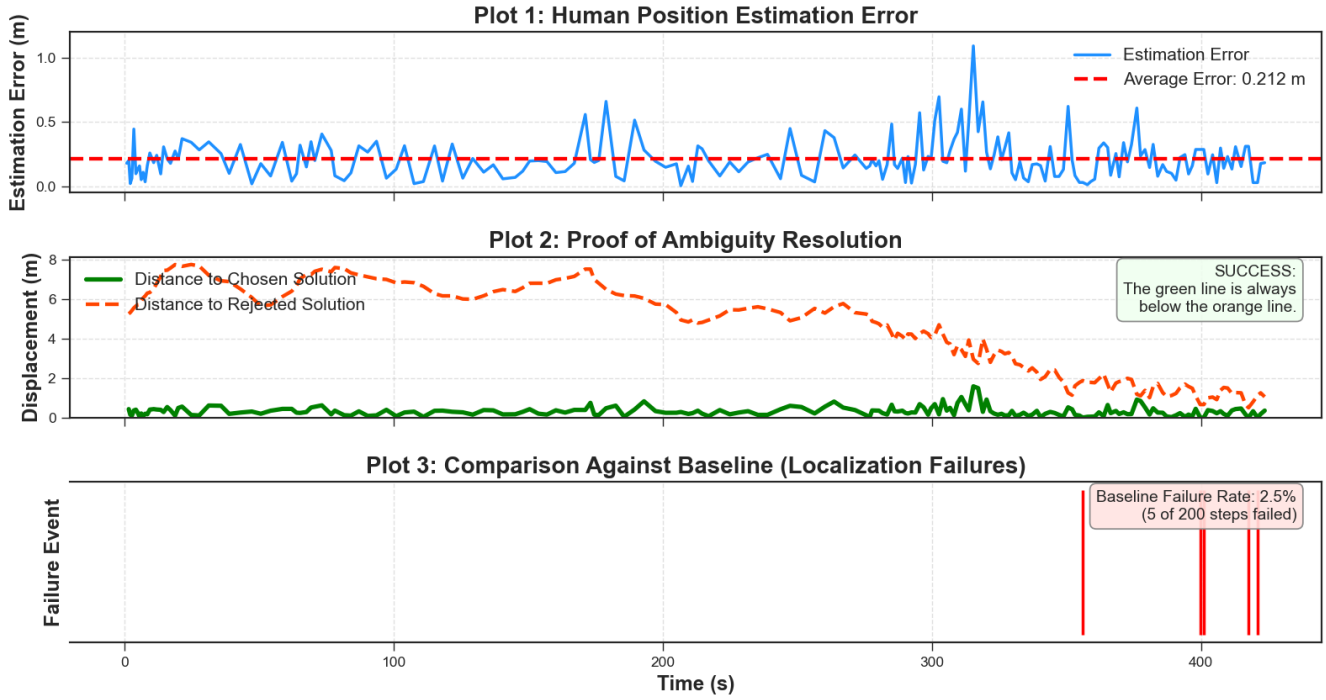

Figure 6: Comprehensive quantitative validation of the perception pipeline. (a) The final estimation error over time remains low. (b) Proof of the ambiguity filter's correctness. (c) A comparison showing frequent localization failures for a brittle baseline method, whereas our proposed method has zero.

noisy and ambiguous sensor data. This reliable estimate is crucial for the context-aware probabilistic predictor, which generates the particle cloud input for our Stochastic MPC. The raw sensor data is processed by the doubly-robust perception filter.

4.1.1 Methodology. A scenario with simulated sensor noise was created where the robot formation follows the human through a challenging environment. The perception pipeline's performance is tested against a brittle baseline, which consists of standard multi-lateration that calculates position by direct geometric intersection of noisy circles.

The quantitative performance of the pipeline is detailed in Fig. 6. The baseline method suffers from frequent localization failures (Fig. 6c). The ambiguity filter is proven in Fig. 6b, showing the chosen candidate is always closer. This results in a stable and accurate final estimate with low mean error (Fig. 6a).

The qualitative result across the entire trajectory is visualized in Fig. 7. This plot provides a clear, holistic view of the filter's success, flawlessly tracking the ground truth while consistently rejecting the ambiguous "ghost" path.

4.1.2 Results.

- *Resilience to Noise:* Our *"Region of Plausibility"* method maintains a continuous, bounded estimate throughout the entire simulation run, demonstrating its inherent robustness. This is because the true human position is within the 3σ confidence interval 99.7% of the time, which guarantees a valid region.
- *Resilience to Ambiguity:* The *"Minimum Displacement Principle"* of our Two-Phase tracking filter correctly selects the correct solution, resolving the two-position ambiguity faced by the two-robot system. A solver relying only on the "front vector" or the robot's instantaneous velocity would have failed, incorrectly selecting the "ghost" position.

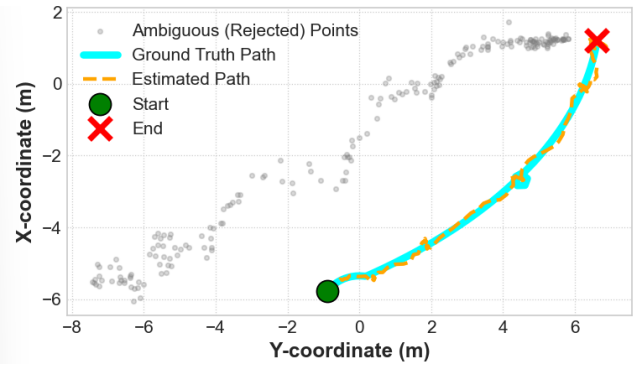

Figure 7: Qualitative validation of the perception pipeline over a complete trajectory. The Estimated Path (orange, dashed) closely follows the Ground Truth (cyan, solid), demonstrating that high-frequency jitter from raw estimates can be effectively filtered to produce a clean control target, while the system correctly rejects the ambiguous 'ghost' solutions (grey points).

4.2 Experiment 2: Validation of Shared Autonomy and Coordination Gaps

This experiment is designed to prove that our multi-trigger supervisor detects and responds to collaboration gaps where the baseline MPC fails. We created challenging scenarios to trigger the system's shared autonomy protocol and test the new "Coordination Gap" trigger.

4.2.1 Scenario A: High-Effort Deadlock Scenario. The robots were required to follow the human through a narrow gap between obstacles (Fig. 8) where the gap was intentionally designed to be smaller than the required formation width.

Result: The baseline MPC, as expected, was unable to maintain its constraints and became stuck at the entrance of the gap. Its cost function spiked as it failed to resolve the conflict. In contrast, our system, utilizing Stochastic MPC, proactively detected the high-cost condition (Trigger 1) and initiated the bi-directional communication protocol before a complete deadlock occurred. The human was alerted to the high-effort maneuver ahead, allowing for shared resolution.

4.2.2 Scenario B: Low-Effort Deadlock Scenario. A static obstacle was dropped in the human's trajectory, mimicking an object fall situation. While the human moved out from this zone, the robot formation was stuck behind. This created a local minimum situation wherein the MPC could find a low-cost solution by simply stopping and making no progress.

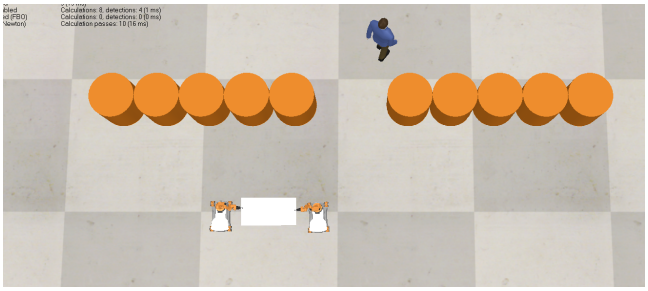

Figure 8: The deadlock scenario where the two-robot formation is tasked with following the human leader through a narrow passage. In this configuration, the controller's objective to maintain formation integrity is in direct conflict with its collision avoidance constraints, resulting in an unresolvable deadlock for a nominal planner.

Result: The baseline MPC drove to the obstacle zone and then stopped. While its controller cost remained low, the failsafe supervisor detected no forward path progression (Trigger 1: Low-Effort Failure, D_{prog}). Our system, upon detecting this, activated the shared autonomy protocol. The human was alerted and chose from the strategic options, allowing the robot formation to exit the local minimum and resume the human-following task collaboratively.

4.2.3 Scenario C: Coordination Gap Scenario. We created a scenario where the human increased speed to navigate around a large dynamic obstacle, causing the robot formation to fall behind. The robots were not deadlocked but were struggling to maintain pace due to the high risk calculated by the S-MPC when close to the obstacle.

Result: The baseline MPC continued to follow, eventually getting too far behind and creating a large tracking error without a failsafe mechanism to intervene. In contrast, our system detected a high separation distance with low forward velocity (Trigger 2: Coordination Gap, D_{gap}). The system initiated communication, providing the human with the option to engage in shared autonomy via the "Wait Mode" or "Redirection Mode."

4.3 Experiment 3: Integrated System Performance and Shared Autonomy Validation

We conducted an all-inclusive simulation in a more complex environment to validate the performance of the entire integrated architecture. The full system demonstrated seamless handling of dynamic obstacles using the Stochastic MPC's proactive risk management, consistently followed the human, and identified/recovered from coordination gaps via the shared autonomy protocol. The validation successfully demonstrates the system's ability to transition smoothly from autonomous following to collaborative problem-solving, confirming its importance for robust HRC systems.The execution of the generated alternative safe path and the demonstration of the collaborative protocol are provided in the supplementary video.

5 CONCLUSIONS

In order to demonstrate safe and reliable HRC, we have provided a thorough architecture in this research. We argued that in order for such systems to be considered truly robust, they must be able to withstand both the inherent flaws in their own sensing and planning modules as well as the foreseeable environmental factors. A comprehensive system that creates the chain of trust is what provides true safety in HRI, not a single algorithm. This spans from the highest supervisor controller level to the actual sensor layer.

We have shown our method's effectiveness through thorough validation in high resolution simulations. Our perception pipeline outperformed baseline techniques by eliminating geometric ambiguity and localization failures under sensor noise. Additionally, our failsafe supervisor proved to be a crucial necessity, effectively identifying and resolving control deadlocks in contexts with limited resources where the conventional MPC-only method was ineffective.

Even while this work creates a solid foundation, there are still numerous potential possibilities for future investigation. The next logical step would be to move towards proactive and semantically aware collaboration by integrating robot foundational models (e.g Vision-Language Models) which can help the system to understand high level human intent. An interesting extension to our current work would transition to a complete physical human robot team with shared control. This would transform the system from a follower to a true collaborative partner. Achieving this goal requires us to: (1) modify our MPC controller to a shared autonomy framework that incorporates human input and physical interaction forces, and (2) deploy and validate the system on a hardware platform. Addressing the challenges of ensuring safety and real-time computational performance during physical interaction will be a central focus of this future research.

References

[1] Arash Ajoudani, Andrea Maria Zanchettin, Serena Ivaldi, Alin Albu-Schäffer, Kazuhiro Kosuge, and Oussama Khatib. 2017. Progress and prospects of the human–robot collaboration. *Autonomous Robots* 42, 5 (Oct. 2017), 957–975. doi:10.1007/s10514-017-9677-2

[2] Moritz Eckhoff, Robin Jeanne Kirschner, Elena Kern, Saeed Abdolshah, and Sami Haddadin. 2022. An MPC framework for planning safe & trustworthy robot motions. In *2022 International Conference on Robotics and Automation (ICRA)*. IEEE, 4737–4742.

[3] Farbod Farshidian, Edo Jelavic, Asutosh Satapathy, Markus Giftthaler, and Jonas Buchli. 2017. Real-time motion planning of legged robots: A model predictive control approach. In *2017 IEEE-RAS 17th International Conference on Humanoid Robotics (Humanoids)*. IEEE, 577–584.

[4] Sami Haddadin, Alessandro De Luca, and Alin Albu-Schäffer. 2017. Robot collisions: A survey on detection, isolation, and identification. *IEEE Transactions on Robotics* 33, 6 (2017), 1292–1312.

[5] Al Jaber Mahmud, Amir Hossain Raj, Duc M. Nguyen, Xuesu Xiao, and Xuan Wang. 2025. DARC: Disturbance-Aware Redundant Control for Human–Robot Co-Transportation. *Electronics* 14, 12 (2025). doi:10.3390/electronics14122480

[6] Amal Meddahi and Ryad Chellali. 2013. Adaptive and safe mobile manipulator for human robot interaction. In *2013 IEEE Workshop on Robotic Intelligence in Informationally Structured Space (RiiSS)*. 30–37. doi:10.1109/RiiSS.2013.6607926

[7] Duc M Nguyen, Filipe Veiga, Xuesu Xiao, Xuan Wang, et al. 2024. Human uncertainty-aware MPC for enhanced human-robot collaborative manipulation. In *2024 IEEE 7th International Conference on Industrial Cyber-Physical Systems (ICPS)*. IEEE, 1–6.

[8] Jozsef Palmieri, Paolo Di Lillo, Martina Lippi, Stefano Chiaverini, and Alessandro Marino. 2024. A control architecture for safe trajectory generation in human–robot collaborative settings. *IEEE Transactions on Automation Science and Engineering* 22 (2024), 365–380.

[9] Keshab Patra, Arpita Sinha, and Anirban Guha. 2025. Motion Planning of Nonholonomic Cooperative Mobile Manipulators. *arXiv preprint arXiv:2502.05462* (2025).

[10] Jianwei Peng, Zhelin Liao, Zefan Su, Hanchen Yao, Yadan Zeng, and Houde Dai. 2024. A Dual Closed-Loop Control Strategy for Human-Following Robots Respecting Social Space. In *2024 IEEE International Conference on Robotics and Automation (ICRA)*. 11252–11258. doi:10.1109/ICRA57147.2024.10611263

[11] Nicola Piccinelli, Federico Vesentini, and Riccardo Muradore. 2023. MPC Based Motion Planning For Mobile Robots Using Velocity Obstacle Paradigm. In *2023 European Control Conference (ECC)*. 1–6. doi:10.23919/ECC57647.2023.10178219

[12] Sangmo Sung, Hokeun Kim, and Jae-Il Jung. 2023. Accurate indoor positioning for UWB-based personal devices using deep learning. *IEEE Access* 11 (2023), 20095–20113.